Asociación Argentina de Mecánica Computacional

Mecánica Computacional Vol XXIX, págs. 1423-1444 (artículo completo)
Eduardo Dvorkin, Marcela Goldschmit, Mario Storti (Eds.)
Buenos Aires, Argentina, 15-18 Noviembre 2010

A FINITE ELEMENT TO PERFORM 3D SHAKEDOWN ANALYSIS FOR LIMITED KINEMATIC HARDENING MATERIALS

Domingos E. S. Nery and Reinaldo J. Jospin

Instituto de Engenharia Nuclear, Comissão Nacional de Energia Nuclear, Rua Helio de Almeida, 75, Cidade Universitaria, Rio de Janeiro, Brasil, domingos@ien.gov.br, rj.jospin@ien.gov.br

Keywords: Limited Kinematic Hardening, Shakedown, Finite Elements.

Abstract. The use of the Design by Analysis (DBA) route is a modern trend in pressure vessel and piping international codes in mechanical engineering. However, to apply the DBA to structures under variable mechanical and thermal loads, it is necessary to assure that the plastic collapse modes, alternate plasticity and incremental collapse (with instantaneous plastic collapse as a particular case), be precluded. The tool available to achieve this target is the shakedown theory. Unfortunately, the practical numerical applications of the shakedown theory result in very large nonlinear optimization problems with nonlinear constraints. Precise, robust and efficient algorithms and finite elements to solve this problem in finite dimension has been a more recent achievements. However, to solve real problems in an industrial level, it is necessary also to consider more realistic material properties as well as to accomplish 3D analysis. Limited kinematic hardening, is a typical property of the usual steels and it should be considered in realistic applications. In this paper, a new finite element with internal thermodynamical variables to model kinematic hardening materials is developed and tested. This element is a mixed ten nodes tetrahedron and through an appropriate change of variables is possible to embed it in a shakedown analysis software developed by Zouain and co-workers for elastic ideally-plastic materials, and then use it to perform 3D shakedown analysis in cases with limited kinematic hardening materials.

1 INTRODUCTION

In many technically meaning structural problems, a possible occurrence of pre existing residual stresses imply that, even if the structure is designed to work in elastic range, eventually at any point, stresses beyond material yield point can occur. Thus, a realistic safety assessment necessarily needs to be done in the pos-yield range. Besides, the loads can varying in time and in each load cycle, plastic deformations occurs, associated with thermal dissipation of internal energy. After unloading, residual stress fields remains and in each new cycle, new different residual stress fields appears. Due to some particular configuration reached by those residual stress fields, after a number of cycles, may occur that the residual stress field staying constant and the dissipation ceases to increase. This stabilization phenomenon is known as shakedown. The critical load below which shakedown can occurs is known as shakedown limit. For loads below this limit, after an initial yielding, the structure starts to behave as elastic being guaranteed its safety relating to the plastic failure. By other side, if a non-shakedown condition occurs, then in each load cycle, the dissipation increase continually and the structure evolve for one of two failure modes: 1) Alternate Plasticity (Low Cycle Fatigue) - (AP) when the dissipation always increase although plastic deformation resulting of the various cycles remains limited. 2) Incremental Collapse (Ratchetting) (IC), when the plastic deformation grows and accumulates in each load cycle. Both failure modes needs to be precluded. A third failure mode known as Instantaneous Plastic Collapse (PC) can occur, if for a single load, the structure becomes a mechanism, with plastic deformation instantly growing without limit. This case can be treated as a particular case of incremental collapse in which, the collapse occurs in the first cycle (Limit Load).

Nowadays design codes prescribes a design philosophy known as "Design by Analysis" (DBA), more general and more compatible with modern analysis technics by the finite element methods. But, to make use of this way of design, it is necessary, beside other requirements, to demonstrate that all plastic collapse modes does not occurs (Mackenzie and Boyle, 1996).

The conditions necessary for shakedown has been theoretically studied for a long time and the theorems related with them (kinematic formulation - Koiter and static formulation - Melan) are one of the most important achievements in the theory of plasticity. Here we will use the static formulation (Melan theorem) for what, it is necessary only to know the extremum values of the loads and the material properties. Although this simplicity, Melan theorem stayed for a long time just as a theoretical reference. Two facts explain this: first, it was deduced based in hypothesis that restricted its applicability in real world as for instance, elastic ideally-plastic materials, small deformations, mechanical properties independent of the temperature and so on. Aiming mitigate this theorem limitations, important developments was made that extends the Melan theorem to deal with real materials, at least from a theoretical point of view. The second fact is that the shakedown analysis is formulated as a very large nonlinear optimization problem with non-linear constraints and to obtain the numerical solution is necessary the availability of robust finite elements and precise and efficient optimization algorithms. Because this fact, only in the last years this tool has becoming available in engineering applications (Staat and Heitzer, 2001). In particular, for the cited case of hardening, Stein et al. (1993) developed an extension of the Melan's theorem. By other side, realistic and general applications frequently requires a 3D analysis.

Seeking the applicability of the shakedown theory to an industrial level, a 3D finite element with internal hardening variable based on Stein's model will be developed for shakedown analysis with limited kinematic hardening. A redefinition of the used variables will be done such that this element can be used embedded in an efficient and precise algorithm developed for the case of elastic ideally-plastic materials by Zouain et al. (2002) to perform shakedown analysis.

2 KINEMATIC AND EQUILIBRIUM

The continuum body is identified with an open and connected region $\mathcal{B}$ of a euclidian space ε^3, with regular boundary Γ, composed of two complementary and disjoint parts, Γ_v where the velocities are prescribed and Γ_τ where traction is prescribed ($\Gamma = \Gamma_v \bigcup \Gamma_\tau$ and $\Gamma_v \bigcap \Gamma_\tau = \emptyset$).

Let $\mathcal{V}$ be the set of all admissible velocity fields v, complying with homogeneous boundary conditions in Γ_v. An operator $\mathcal{D}$, over $\mathcal{V}$, maps $\mathcal{V}$ into the space $\mathcal{W}$, of strain rates tensor fields ε and it is called tangent deformation operator. Let $\mathcal{W}'$ be the space of stress fields σ and $\mathcal{V}'$ the space of load systems, F. $\mathcal{W}'$ is mapped into $\mathcal{V}'$ by the equilibrium operator $\mathcal{D}'$, dual of $\mathcal{D}$. The kinematical and equilibrium relations are written as:

$$\varepsilon = \mathcal{D}v \qquad F = \mathcal{D}'\sigma \tag{1}$$

The duality product between $\mathcal{W}'$ and $\mathcal{W}$, defines for each pair $\sigma \in \mathcal{W}'$ e $\varepsilon \in \mathcal{W}$ a bi-linear functional, the internal power.

$$\langle \sigma, \varepsilon \rangle = \int_{\mathcal{B}} \sigma \cdot \varepsilon \, d\mathcal{B} \tag{2}$$

The duality product between $\mathcal{V}$ and $\mathcal{V}'$ is the external power defined by the linear functional in v:

$$\langle F, v \rangle = \int_{\mathcal{B}} b \cdot v \, d\mathcal{B} + \int_{\Gamma_\tau} \tau \cdot v \, d\Gamma \tag{3}$$

where the load systems are unfolded in body forces b and traction τ, in Γ_τ. The virtual power principle is written as:

$$\langle \sigma, \mathcal{D}v \rangle = \langle F, v \rangle, \qquad \forall v \in \mathcal{V} \tag{4}$$

3 CONSTITUTIVE RELATIONS

3.1 State variables

To assure physical consistency and adequate formalism we make use of the thermodynamic of continuous media to derive the constitutive relations. The standard generalized material model (Halphen and Nguyen, 1975), (Maugin, 1992) is adopted here and small deformations is considered. The local states method (Lemaitre and Chaboche, 1990), p.57. is used and, aiming to consider kinematic hardening, the following generalized state variables are adopted:

$$\begin{aligned}
\boldsymbol{\varepsilon} &= (\varepsilon, 0) && \text{generalized strain}\\
\boldsymbol{\varepsilon}^e &= (\varepsilon^e, \omega) && \text{generalized reversible strain}\\
\boldsymbol{\varepsilon}^p &= (\varepsilon^p, \beta) && \text{generalized irreversible strain}\\
\boldsymbol{\sigma} &= (\sigma, A) && \text{generalized stress}
\end{aligned}$$

where, ε is the total strain, ε^e is the thermo-elastic strain, ε^p is the plastic strain, β is the irreversible internal hardening variable, ω is the reversible internal hardening variable, σ is the Cauchy stress tensor and A is the back stress.

With additive decomposition of strain we have $\boldsymbol{\varepsilon} = \boldsymbol{\varepsilon}^e + \boldsymbol{\varepsilon}^p$ and then:

$$\varepsilon = \varepsilon^e + \varepsilon^p \tag{5}$$

$$0 = \omega + \beta \qquad \Longrightarrow \omega = -\beta \tag{6}$$

In small deformations, as usual, we call $d^p = \dot{\varepsilon}^p$. The kinematical relations is written

$$\boldsymbol{\varepsilon} = \boldsymbol{\mathcal{D}} v \tag{7}$$

with

$$\boldsymbol{\mathcal{D}} = \begin{bmatrix} \mathcal{D} \\ \boldsymbol{0} \end{bmatrix} \tag{8}$$

where $\boldsymbol{\mathcal{D}}$ is a strain deformation operator considering the generalized variables.

3.2 State laws

Let θ be the atual temperature and θ_0 a reference temperature. Let's suppose that $(\theta - \theta_0)$ is small compared to θ_0 and that slow heating process occur. In this condition, the process can be considered approximately isothermal ($\dot{\theta} \simeq 0$). Due this fact, the state laws for the thermo-elastic problem can be derived from a thermodynamical potential $\Psi(\varepsilon^e, \beta)$, quadratic and positive defined, where the elastic and thermal terms are uncoupled (Matt and Borges, 2001). As elasticity and hardening are also uncoupled the potential is written:

$$\Psi(\varepsilon^e, \beta) = \int_{\mathcal{B}} \left\{ \frac{1}{2} \mathbb{E} \varepsilon^e \varepsilon^e - \frac{E}{(1-2\nu)} \mathrm{tr}(\varepsilon^e) \alpha \theta - \frac{c_\epsilon}{2\theta_0} \theta^2 + \frac{1}{2} \mathbb{H} \beta \beta \right\} d\mathcal{B} \tag{9}$$

The inverse state law can be obtained from a dual thermodynamical potential $\Psi^c(\sigma, A)$ obtained by a Legendre-Fenchel transformation of Ψ (Matt and Borges, 2001):

$$\Psi^c(\sigma, A) = \int_{\mathcal{B}} \left\{ \frac{1}{2} \mathbb{E}^{-1} \sigma\sigma + \alpha\theta \mathrm{tr}(\sigma) + \left(\frac{3E}{(1-2\nu)} \alpha^2 + \frac{c_\epsilon}{\theta_0} \right) \frac{\theta^2}{2} + \frac{1}{2} \mathbb{H}^{-1} A A \right\} d\mathcal{B} \tag{10}$$

$$\mathbb{E} = \frac{E}{(1+\nu)} \boldsymbol{I\!I} + \frac{E\nu}{(1+\nu)(1-2\nu)} (\boldsymbol{I} \otimes \boldsymbol{I}) \quad , \quad \mathbb{E}^{-1} = \frac{(1+\nu)}{E} \boldsymbol{I\!I} - \frac{\nu}{E} (\boldsymbol{I} \otimes \boldsymbol{I}) \tag{11}$$

and assuming linear hardening

$$\mathbb{H} = h\mathbb{E} \quad , \quad \mathbb{H}^{-1} = \frac{1}{h} \mathbb{E}^{-1} \tag{12}$$

Here, E is the Young modulus, ν is the Poisson coefficient, α is the thermal expansion coefficient, c_ϵ is the strain specific heat constant, h is a proportionality factor and $\boldsymbol{I\!I}$ and $\boldsymbol{I}$ are respectively the identity forth and second order tensors.

The state laws derived from that potentials are:

$$\sigma = \nabla_{\varepsilon^e} \Psi(\varepsilon^e, \beta) \quad \Longleftrightarrow \quad \varepsilon^e = \nabla^c_\sigma \Psi(\sigma, A) \tag{13}$$

$$A = -\nabla_\beta \Psi(\varepsilon^e, \beta) \quad \Longleftrightarrow \quad \beta = -\nabla^c_A \Psi(\sigma, A) \tag{14}$$

As ε^e and β are uncoupled, the state laws becomes:

$$\sigma = \mathbb{E} \varepsilon^e - \frac{E}{(1-2\nu)} \alpha\theta \boldsymbol{I} \quad \Longleftrightarrow \quad \varepsilon = \mathbb{E}^{-1} \sigma + \alpha\theta \boldsymbol{I} \tag{15}$$

and

$$A = -\mathbb{H}\beta \quad \Longleftrightarrow \quad \beta = -\mathbb{H}^{-1} A \tag{16}$$

with $\mathbb{E}$ and $\mathbb{H}$ linear operators.

3.3 Flow Laws

The evolution laws are derived from a dissipation potential defined by Hill's maximum dissipation principle:

$$\chi(d^p, \dot{\beta}) = \sup_{(\sigma^*, A^*) \in P} (\sigma^* \cdot d^p + A^* \cdot \dot{\beta}) \tag{17}$$

where P is the plastic admissibility domain.

Let $\mathcal{I}_P(\sigma, A)$ be the indicator function of P, that equals zero for $(\sigma^*, A^*) \in P$ and $+\infty$ otherwise. Then, the dissipation χ can be written:

$$\chi(d^p, \dot{\beta}) = \sup_{(\sigma^*, A^*)} \{\sigma^* \cdot d^p + A^* \cdot \dot{\beta} - \mathcal{I}_P(\sigma, A)\} \tag{18}$$

not being χ Fréchet differentiable. For the case of the associative plastic flow, the constitutive relations between plastic strain rates $(d^P, \dot{\beta})$ and stresses (σ, A) are written:

$$(\sigma, A) \in \partial\chi(d^p, \dot{\beta}) \Leftrightarrow (d^p, \dot{\beta}) \in N_P(\sigma, A) \tag{19}$$

where $\partial\chi$ represents the sub-differential set of χ, defined by:

$$\chi^*(d^p, \dot{\beta}) - \chi(d^p, \dot{\beta}) \geq (\sigma, A) \cdot [(d^p, \dot{\beta})^* - (d^p, \dot{\beta})] \quad , \quad \forall (d^p, \dot{\beta})^* \tag{20}$$

and $N_P(\sigma, A) := \partial\mathcal{I}_P(\sigma, A)$ is the cone of normals to yield surface P in σ, i.e. the set of all plastic strain rates (d^P, β) such as

$$(\sigma - \sigma^*) \cdot d^p + (A - A^*) \cdot \dot{\beta} \leq 0 \quad , \quad \forall\ (\sigma^*, A^*) \in P \tag{21}$$

The dissipation function is a support function of P, hence it is sub-linear, i.e. convex and positive homogeneous of first degree. It also satisfies $\chi(0, 0) \geq 0$ because $(\sigma, A) = 0 \in P$. In the case of Mises criteria, f is unimodal and regular and for generalized standard materials, the relations (19) are equivalent to the classical form:

$$(d^p, \dot{\beta}) = \dot{\lambda} \nabla f(\sigma, A) \tag{22}$$

Here $\nabla f(\sigma, A)$ denotes the gradient of f and $\dot{\lambda}$ is a m-vector field of plastic multipliers. At any point in $\mathcal{B}$, the components of $\dot{\lambda}$ are related to each plastic mode in f by the complementarity conditions:

$$\dot{\lambda} f(\sigma, A) = 0 \quad f(\sigma, A) \leq 0 \quad \dot{\lambda} \geq 0 \tag{23}$$

(this inequalities hold componentwise).

4 SHAKEDOWN ANALYSIS

4.1 Load domain

Shakedown analysis needs only the materials properties and a prescribed domain Δ^0 in load space defined by the extremum loads containing any feasible load history. However, it is more convenient to mapping this domain in a correspondent domain Δ^E in elastic stress space, to dealing with the mechanical and thermal loads in a same framework. The domain Δ^E is assumed to be convex and bounded. Any interior point of polyhedron Δ^E is a convex combination of its vertex. If a non-linear dependence between the loads exists, a function that defines the load coupling must be discretized. To avoid this, it is still convenient to consider the total uncoupling of loads defining a local uncoupled envelope Δ which collect the extremum values of stresses corresponding to the loads in each body point, independently of position of the stress point in the load cycle. Consider the set of all the local values of elastic stresses associated to any feasible loading, i.e

$$\forall x \in \mathcal{B}, \quad \Delta(x) := \{\sigma^E(x) \quad | \quad \forall \sigma^E \in \Delta^E\} \tag{24}$$

The pointwise envelope Δ of set Δ^E is

$$\Delta := \{\sigma \quad | \quad \sigma(x) \in \Delta(x), \quad \forall x \in \mathcal{B}\} \supset \Delta^E \tag{25}$$

4.2 Shakedown and limited kinematical hardening

The theorem due to Bleich-Melan states that any load factor μ^* is safe if there exists a time-independent residual (self-equilibrated) stress field σ^r such that its superposition with any stress belonging to the amplified load domain $\mu^*\Delta$ is plastically admissible. Then, for elastic shakedown, the limit load factor μ is the supremum of all safe factors. This may be translated as an elastic shakedown equilibrium variational principle:

$$\mu := \sup_{(\mu^*,\sigma^r)\in\mathbb{R}\times\mathcal{W}'} \{\mu^* \geq 0 \quad | \quad \mu^*\Delta + \sigma^r \subset P, \qquad \sigma^r \in S^r\} \tag{26}$$

Stein et al. (1990), Stein et al. (1992) and Stein et al. (1993), studied a shakedown behavior of kinematic hardening materials bodies using a 3D overlay model for reproduce hardening. The main idea was to approach the behavior of metals by a composite of elastic-ideally plastic micro-elements in a dense spectrum, numbered with a scalar variable $\xi \in [0, 1]$ and deforming together.

Let

$$\Phi(\boldsymbol{\sigma}) := \frac{3}{2}\|\mathbf{S}\|^2 \tag{27}$$

be the homogeneous part of Mises yield function. Here the generalized stress deviator is $\mathbf{S} = (S, A)$.

Stein's work shown that the theorem of Melan can be stated for materials with hardening, in terms of the back stress A as: If exist a load factor $m > 1$, a time independent residual stress field, $\sigma^r(x) \in S^r$ and a time-independent back stress field $A(x, \xi)$ satisfying

$$\Phi(A(x, 0)) \leq [\sigma_Y(x) - \sigma_{Y0}(x)]^2 \tag{28}$$

such as for all possible loads in the load domain, the condition

$$\Phi(m\sigma^E(x, t) + \sigma^r(x) - A(x, 0)) \leq [\sigma_{Y0}(x)]^2 \tag{29}$$

is fulfilled $\forall x \in \beta$ and $\forall t \geq 0$, where $m > 1$ is a safety factor against non shakedown, then the total plastic energy dissipated within an arbitrary load path contained within the load domain is bounded. Here, σ_Y is a yield stress in the end of hardening and σ_{Y0} is the initial yield stress. This model does not depends on the shape of the hardening curve and because this fact, in spit of we consider here linear hardening, the resulting shakedown factors are valid for any hardening curve shape. The correspondent statical principle is:

$$\mu = \sup_{(\mu^*,\sigma^r,A)\in\mathbb{R}\times\mathcal{W}'\times\mathcal{W}'} \{\mu^* \leq 0 \mid \Phi(\mu^*\sigma^E + \sigma^r - A) \leq \sigma_{Y0}^2; \Phi(A) \leq (\sigma_Y - \sigma_{Y0})^2; \sigma^r \in S^r\} \tag{30}$$

The yield functions corresponding to the conditions of Stein's statement are:

$$f_{S1}(\sigma, A) = \frac{3}{2}\|S - A^{dev}\|^2 - (\sigma_{Y0})^2 \tag{31}$$

$$f_{S2}(A) = \frac{3}{2}\|A^{dev}\|^2 - (\sigma_Y - \sigma_{Y0})^2 \tag{32}$$

From the static principle (30), a mixed and a kinematical principles can be derived (Zouain et al., 2002), (Zouain, 2004). Anyone of this principles or their optimality conditions can motivate a discretization for the numerical solution.

Let's consider the whole set of constraints in the mixed principle for the n_{elem} elements mesh. The plastic admissibility has to be imposed in p points (stress vertices) in each elements for each basic load n_Δ of the load domain. As the load domain Δ is convex and the stress interpolation will be linear, then will be necessary to enforce plastic admissibility only at the triangle vertices to assure this condition over the whole element. Thus, there are pn_{elem} points in the mesh where plastic admissibility is explicitly enforced for each basic load. This results, for the Stein's bimodal yield surface in $m := 2pn_{\text{elem}}n_\Delta$ inequality constraints, that are enumerated using a single index $k = 1 : m$ in correspondence to (ℓ, i, j) with $\ell = 1, n_\Delta$, $i = 1 : 2$ and $j = 1 : p\, n_{\text{elem}}$. The discrete optimality conditions considering limited hardening with internal variables can be stated as follows (Nery, 2007), considering $\sum := \sum_{k=1:m}$:

$$B^T \sigma^r = 0 \tag{33}$$

$$\sum d^k = Bv \tag{34}$$

$$\sum \dot{\beta}^k + \dot{\beta}^A = 0 \tag{35}$$

$$\sum \sigma^k \cdot d^k = 1 \tag{36}$$

$$d^k = \dot{\lambda}^k \nabla_\sigma f^k \qquad k = 1 : m \tag{37}$$

$$\dot{\beta}^k = \dot{\lambda}^k \nabla_A f^k \qquad k = 1 : m \tag{38}$$

$$\dot{\beta}^A = \dot{\lambda}^A \nabla_A f^A \tag{39}$$

$$\dot{\lambda}^k f^k = 0 \qquad k = 1 : m \tag{40}$$

$$\dot{\lambda}^A f^A = 0 \tag{41}$$

$$f^k := f_{S1}(\mu\sigma^k + \sigma^r, A) \leq 0 \qquad k = 1 : m \tag{42}$$

$$f^A := f_{S2}(A) \leq 0 \tag{43}$$

$$\dot{\lambda}^k \geq 0 \qquad k = 1 : m \tag{44}$$

$$\dot{\lambda}^A \geq 0 \tag{45}$$

To solve the shakedown problems in case of hardening one needs to find:

$$\{v, \sigma^r, A, \mu, \dot{\lambda}^k, \dot{\lambda}^A\} \tag{46}$$

The algorithm developed for elastic ideally-plastic materials by Zouain et al. (2002), Zouain (2004) can be adapted, to solve shakedown problem with limited kinematic hardening (Nery, 2007). For to do this, the internal variable A will be considered together with the residual stress in a vector, but not constrained to be residual and the discrete deformation operator B will be constructed to have null elements in the positions corresponding to the internal variables. The new vectors that will be considered to be used in Zouain's algorithm, to taking into account the limited kinematic hardening are:

$$\boldsymbol{\sigma}^r = (\sigma^r, A) \qquad \boldsymbol{d}^k = (d^k, \dot{\beta}^k) \qquad \boldsymbol{\sigma}^k = (\sigma^k, 0) \qquad \dot{\boldsymbol{\lambda}}^k = (\dot{\lambda}^k, \dot{\lambda}^A) \tag{47}$$

With this definitions, the discrete optimality conditions are written:

$$B^T \boldsymbol{\sigma}^r = 0 \tag{48}$$

$$\sum \dot{\boldsymbol{\lambda}}^k \nabla_{\boldsymbol{\sigma}} f^k = Bv \tag{49}$$

$$\sum \boldsymbol{\sigma}^k \cdot \dot{\boldsymbol{\lambda}}^k \nabla_{\boldsymbol{\sigma}} f^k = 1 \tag{50}$$

$$\dot{\boldsymbol{\lambda}}^k f^k = 0 \qquad k = 1:m \tag{51}$$

$$f^k := f_{S1}(\mu\boldsymbol{\sigma}^k + \boldsymbol{\sigma}^{\boldsymbol{r}}) \leq 0 \qquad k = 1:m \tag{52}$$

$$f^A := f_{S2}(A) \leq 0 \tag{53}$$

$$\dot{\boldsymbol{\lambda}}^k \geq 0 \qquad k = 1:m \tag{54}$$

Then, with this change of variables, the same algorithm developed for elastic ideally-plastic materials (Zouain et al., 2002), (Zouain, 2004) can be used for materials with limited kinematic hardening, considering additionally the plastic admissibility constraint (53).

5 MIXED TETRAHEDRON FINITE ELEMENT FOR 3D SHAKEDOWN ANALYSIS WITH LIMITED KINEMATIC HARDENING INTERNAL VARIABLE

In finite dimension, the discretization in finite elements was done using a ten nodes mixed two fields (v and $\boldsymbol{\sigma}$) tetrahedron. The velocity field is quadratically interpolated with C^0 continuity between elements. The stress field is linearly interpolated and the internal variable field is constant inside the element, both with inter-element discontinuities. Due to this linear stress interpolation and to the convexity of the load domain, it is necessary to verify the plastic admissibility only in the four stress nodes of the tetrahedron to assure the plastic admissibility over all the element. In the following, the bold symbols stands for generalized variables and related operators and not for tensors as usual.

5.1 Macroscopic and internal 3D variables

$$v := \begin{bmatrix} v_x \; v_y \; v_z \end{bmatrix}^T \tag{55}$$

The second order symmetrical tensor can be represented on a six dimension vector space with a six second order tensor basis. This representation results:

$$\boldsymbol{\varepsilon} := \begin{bmatrix} \varepsilon_x \; \varepsilon_y \; \varepsilon_z \; \varepsilon_{(xy)} \; \varepsilon_{(xz)} \; \varepsilon_{(yz)} \; \beta_x \; \beta_y \; \beta_z \; \beta_{(xy)} \; \beta_{(xz)} \; \beta_{(yz)} \end{bmatrix}^T \tag{56}$$

$$\boldsymbol{d} := \begin{bmatrix} d_x \; d_y \; d_z \; d_{(xy)} \; d_{(xz)} \; d_{(yz)} \; \dot{\beta}_x \; \dot{\beta}_y \; \dot{\beta}_z \; \dot{\beta}_{(xy)} \; \dot{\beta}_{(xz)} \; \dot{\beta}_{(yz)} \end{bmatrix}^T \tag{57}$$

$$\boldsymbol{\sigma} := \begin{bmatrix} \sigma_x \; \sigma_y \; \sigma_z \; \sigma_{(xy)} \; \sigma_{(xz)} \; \sigma_{(yz)} \; A_x \; A_y \; A_z \; A_{(xy)} \; A_{(xz)} \; A_{(yz)} \end{bmatrix}^T \tag{58}$$

where $\varepsilon_{(xy)} = \sqrt{2}\varepsilon_{xy}$, the same notation been valid for the other shear components. The compatible strains operator is:

$$\boldsymbol{D} := \begin{bmatrix} D \\ 0 \end{bmatrix} \tag{59}$$

where the null positions corresponds to the internal variable components.

$$\boldsymbol{D} := \begin{bmatrix} \partial_x & 0 & 0 \\ 0 & \partial_y & 0 \\ 0 & 0 & \partial_z \\ \frac{1}{\sqrt{2}}\partial_y & \frac{1}{\sqrt{2}}\partial_x & 0 \\ \frac{1}{\sqrt{2}}\partial_z & 0 & \frac{1}{\sqrt{2}}\partial_x \\ 0 & \frac{1}{\sqrt{2}}\partial_z & \frac{1}{\sqrt{2}}\partial_y \\ 0_{6\times1} & 0_{6\times1} & 0_{6\times1} \end{bmatrix} \tag{60}$$

The elastic relation is:

$$\mathbb{E} := \begin{bmatrix} \mathbb{E} & 0 \\ 0 & \mathbb{H} \end{bmatrix} \tag{61}$$

where

$$\mathbb{E} = m = \frac{E}{(1+\nu)(1-2\nu)} \begin{bmatrix} 1-\nu & \nu & \nu & 0 & 0 & 0 \\ \nu & 1-\nu & \nu & 0 & 0 & 0 \\ \nu & \nu & 1-\nu & 0 & 0 & 0 \\ 0 & 0 & 0 & 1-2\nu & 0 & 0 \\ 0 & 0 & 0 & 0 & 1-2\nu & 0 \\ 0 & 0 & 0 & 0 & 0 & 1-2\nu \end{bmatrix} \tag{62}$$

with thermal deformation:

$$\varepsilon^{\theta} = \alpha\theta\,[1\ 1\ 1\ 0\ 0\ 0]^T \tag{63}$$

and

$$\mathbb{E}^{-1} = n = \frac{1}{E} \begin{bmatrix} 1 & -\nu & -\nu & 0 & 0 & 0 \\ -\nu & 1 & -\nu & 0 & 0 & 0 \\ -\nu & -\nu & 1 & 0 & 0 & 0 \\ 0 & 0 & 0 & 1+\nu & 0 & 0 \\ 0 & 0 & 0 & 0 & 1+\nu & 0 \\ 0 & 0 & 0 & 0 & 0 & 1+\nu \end{bmatrix} \tag{64}$$

The Stein's model, used here to calculate the shakedown factor depends only on the initial and final yield stresses. So, the results are independent on the shape of the hardening curve. We assume linear hardening $H = hE$, and $\mathbb{H} = h\mathbb{E}$ in elastic range, where h is a proportionality factor.

5.2 The finite element

5.2.1 Variational principle for thermo-elasticity

For thermo-elasticity, a mixed two fields (velocities and stresses) variational principle referred as Hellinger-Reissner principle is obtained from the thermodynamic potentials Eqs.(9) and (10) (Matt and Borges, 2001). The variational statement is:

Find $v \in V$ and $\sigma \in W'$ such that

$$\Pi^{HR}(v,\boldsymbol{\sigma}) = \inf_{v^* \in V^0} \sup_{\boldsymbol{\sigma}^{**} \in W'} \left[-\frac{1}{2} \int_{\mathcal{B}} \boldsymbol{\sigma}^{**} \mathbb{E}^{-1} \boldsymbol{\sigma}^{**} \, d\mathcal{B} + \int_{\mathcal{B}} \boldsymbol{\sigma}^{**} \mathcal{D} v^* \, d\mathcal{B} - \int_{\mathcal{B}} \boldsymbol{F} v^* \, d\mathcal{B} - \int_{\mathcal{B}} \alpha \theta \, \mathrm{tr}(\boldsymbol{\sigma}^{**}) \, d\mathcal{B} - \int_{\Gamma_\tau} \bar{t} v^* \, d\mathcal{B} \right. \quad (65)$$

where $\mathbb{E}^{-1}$ is defined by Eq. (61). The velocities, stresses and temperature are interpolated in the element;

$$v = \boldsymbol{N}_v v^n \quad , \quad \boldsymbol{\sigma} = \boldsymbol{N}_\sigma \boldsymbol{\sigma}^n \quad , \quad \theta = \boldsymbol{N}_\theta \theta^n \quad (66)$$

where the $\boldsymbol{N_v}$ and $\boldsymbol{N_\theta}$ represents the quadratic (for velocities and temperature respectively) and $\boldsymbol{N_\sigma}$ linear (for stresses) Lagrangian interpolation operators. The vectors v^e, $\boldsymbol{\sigma}^e$ and θ^e are the interpolation parameters for the element e. The discrete Hellinger-Reissner principle can be written (Matt and Borges, 2001):

$$\Pi^{HR}(v,\boldsymbol{\sigma}) = \min_{v^* \in R^s} \max_{\boldsymbol{\sigma}^{**} \in R^q} \left[-\frac{1}{2} \mathbb{E}^{-1} \boldsymbol{\sigma}^{**} \cdot \boldsymbol{\sigma}^{**} + \boldsymbol{\sigma}^{**} \cdot \boldsymbol{B} \, v^* - \boldsymbol{F} \cdot v^* - \boldsymbol{\sigma}^{**} \cdot \boldsymbol{\Theta} - \bar{t} \cdot v^* \right] \quad (67)$$

where s is the number of velocity degrees of freedom and q is total number of stress parameters which in this case is twenty four times the total number of elements because the stresses will be considered discontinuous between the elements. In Eq. 67 the contribution of each element to be assembled are:

$$\mathbb{E}^{-1^e} = \int_{\beta^e} \boldsymbol{N}_\sigma^T \mathbb{E}^{-1} \boldsymbol{N}_\sigma \, d\beta \qquad \boldsymbol{B}^e = \int_{\beta^e} \boldsymbol{N}_\sigma^T \boldsymbol{D} \boldsymbol{N}_v \, d\beta \quad (68)$$

$$\boldsymbol{F}^e = \int_{\beta^e} \boldsymbol{N}_v^T \, b \, d\beta + \int_{\Gamma_\tau^e} \boldsymbol{N}_v^T \, \bar{t} \, d\Gamma_\tau \qquad \boldsymbol{\Theta}^e = \int_{\beta^e} \alpha \boldsymbol{N}_\sigma^T \boldsymbol{I} \boldsymbol{N}_v \theta^e \, d\beta \quad (69)$$

Calculating the first variation of Eq. (67), this min-max problem solution is equivalent to solve the equation set:

$$\mathbb{E}^{-1} \boldsymbol{\sigma} - \boldsymbol{B} v + \boldsymbol{\Theta} = 0 \quad (70)$$

$$\boldsymbol{B}^T \boldsymbol{\sigma} - \boldsymbol{F} = 0 \quad (71)$$

with

$$t = \bar{t} \in \Gamma_\tau \quad (72)$$

5.2.2 Interpolation functions

The linear interpolation functions used for stresses are:

$$\ell_1 = \kappa \quad (73)$$

$$\ell_2 = \xi \quad (74)$$

$$\ell_3 = \eta \quad (75)$$

$$\ell_4 = \zeta \quad (76)$$

where

$$\kappa = 1 - \xi - \eta - \zeta \quad (77)$$

and for velocities and temperature, the quadratic interpolation functions are used:

$$g_1 = \kappa(2\kappa - 1) \tag{78}$$
$$g_2 = \xi(2\xi - 1) \tag{79}$$
$$g_3 = \eta(2\eta - 1) \tag{80}$$
$$g_4 = \zeta(2\zeta - 1) \tag{81}$$
$$g_5 = 4\xi\kappa \tag{82}$$
$$g_6 = 4\xi\eta \tag{83}$$
$$g_7 = 4\eta\kappa \tag{84}$$
$$g_8 = 4\zeta\kappa \tag{85}$$
$$g_9 = 4\xi\zeta \tag{86}$$
$$g_{10} = 4\eta\zeta \tag{87}$$

The internal variables are constant in the element.

5.2.3 Interpolation operators

The velocity components in the ten nodes tetrahedron are:

$$v^i = \left[v_x^1\ v_y^1\ v_z^1 \ldots\ v_x^{10}\ v_y^{10}\ v_z^{10}\right]^T \in I\!R^{30} \tag{88}$$

and for this element the interpolation function matrix for velocities and temperature are:

$$\boldsymbol{N}_v \;=\; \left[g_1 \boldsymbol{1}_3 \quad \ldots \quad g_{10} \boldsymbol{1}_3\right] \in I\!R^{3\times 30} \tag{89}$$

and

$$\boldsymbol{N}_\theta \;=\; \left[g_1 \quad \ldots \quad g_{10}\right] \in I\!R^{10} \tag{90}$$

For the k stress nodes we have:

$$\boldsymbol{\varepsilon}^i := \left[\varepsilon_x^k\ \varepsilon_y^k\ \varepsilon_z^k\ \varepsilon_{(xy)}^k\ \varepsilon_{(xz)}^k\ \varepsilon_{(yz)}^k\ \beta_x\ \beta_y\ \beta_z\ \beta_{(xy)}\ \beta_{(xz)}\ \beta_{(yz)}\right]^T \in I\!R^{30} \tag{91}$$

$$\boldsymbol{d}^i := \left[d_x^k\ d_y^k\ d_z^k\ d_{(xy)}^k\ d_{(xz)}^k\ d_{(yz)}^k\ \dot\beta_x\ \dot\beta_y\ \dot\beta_z\ \dot\beta_{(xy)}\ \dot\beta_{(xz)}\ \dot\beta_{(yz)}\right]^T \in I\!R^{30} \tag{92}$$

$$\boldsymbol{\sigma}^i := \left[\sigma_x^k\ \sigma_y^k\ \sigma_z^k\ \sigma_{(xy)}^k\ \sigma_{(xz)}^k\ \sigma_{(yz)}^k\ A_x\ A_y\ A_z\ A_{(xy)}\ A_{(xz)}\ A_{(yz)}\right]^T \in I\!R^{30} \tag{93}$$

with k varying from 1 to 4.

$$\boldsymbol{N}_\sigma = \begin{bmatrix} \ell_1 \mathit{1}_6 & \ell_2 \mathit{1}_6 & \ell_3 \mathit{1}_6 & \ell_4 \mathit{1}_6 & \mathit{0}_{6\times 6} \\ \mathit{0}_{6\times 6} & \mathit{0}_{6\times 6} & \mathit{0}_{6\times 6} & \mathit{0}_{6\times 6} & \mathit{1}_6 \end{bmatrix} \in I\!R^{12\times 30} \tag{94}$$

Here, the symbol $\mathit{0}_{i\times j}$ stands for a matrix with i lines and j columns of null positions and the symbol $\mathit{1}_i$ stands for a unit diagonal matrix with i positions.

5.2.4 Discrete strain operator

Let β^e be the element volume. The discrete strain operator is obtained from the relation:

$$\boldsymbol{B} = \int_{\beta^e} \boldsymbol{N}_\sigma^T \boldsymbol{D} \boldsymbol{N}_v \, d\beta = \begin{bmatrix} B^1 & \dots & B^{10} \end{bmatrix} \in I\!R^{30\times 30} \tag{95}$$

where

$$\boldsymbol{N}_v = \begin{bmatrix} \mathsf{B}^1 & \dots & \mathsf{B}^{10} \end{bmatrix} \in I\!R^{12\times 30} \tag{96}$$

$$\mathsf{B}^k = \begin{bmatrix} g_{k,x} & 0 & 0 \\ 0 & g_{k,y} & 0 \\ 0 & 0 & g_{k,z} \\ \frac{1}{\sqrt{2}}\, g_{k,y} & \frac{1}{\sqrt{2}}\, g_{k,x} & 0 \\ \frac{1}{\sqrt{2}}\, g_{k,z} & 0 & \frac{1}{\sqrt{2}}\, g_{k,x} \\ 0 & \frac{1}{\sqrt{2}}\, g_{k,z} & \frac{1}{\sqrt{2}}\, g_{k,y} \\ 0_{6\times 1} & 0_{6\times 1} & 0_{6\times 1} \end{bmatrix} \in I\!R^{12\times 3} \tag{97}$$

and, for k varying from 1 to 10

$$\boldsymbol{B}^k = \int_{\beta^e} \left[\begin{array}{ccc} \ell_1\, g_{k,x} & 0 & 0 \\ 0 & \ell_1\, g_{k,y} & 0 \\ 0 & 0 & \ell_1\, g_{k,z} \\ \frac{1}{\sqrt{2}}\, \ell_1\, g_{k,y} & \frac{1}{\sqrt{2}}\, \ell_1\, g_{k,x} & 0 \\ \frac{1}{\sqrt{2}}\, \ell_1\, g_{k,z} & 0 & \frac{1}{\sqrt{2}}\, \ell_1\, g_{k,x} \\ 0 & \frac{1}{\sqrt{2}}\, \ell_1\, g_{k,z} & \frac{1}{\sqrt{2}}\, \ell_1\, g_{k,y} \\ \hline \ell_2\, g_{k,x} & 0 & 0 \\ 0 & \ell_2\, g_{k,y} & 0 \\ 0 & 0 & \ell_2\, g_{k,z} \\ \frac{1}{\sqrt{2}}\, \ell_2\, g_{k,y} & \frac{1}{\sqrt{2}}\, \ell_2\, g_{k,x} & 0 \\ \frac{1}{\sqrt{2}}\, \ell_2\, g_{k,z} & 0 & \frac{1}{\sqrt{2}}\, \ell_2\, g_{k,x} \\ 0 & \frac{1}{\sqrt{2}}\, \ell_2\, g_{k,z} & \frac{1}{\sqrt{2}}\, \ell_2\, g_{k,y} \\ \hline \ell_3\, g_{k,x} & 0 & 0 \\ 0 & \ell_3\, g_{k,y} & 0 \\ 0 & 0 & \ell_3\, g_{k,z} \\ \frac{1}{\sqrt{2}}\, \ell_3\, g_{k,y} & \frac{1}{\sqrt{2}}\, \ell_3\, g_{k,x} & 0 \\ \frac{1}{\sqrt{2}}\, \ell_3\, g_{k,z} & 0 & \frac{1}{\sqrt{2}}\, \ell_3\, g_{k,x} \\ 0 & \frac{1}{\sqrt{2}}\, \ell_3\, g_{k,z} & \frac{1}{\sqrt{2}}\, \ell_3\, g_{k,y} \\ \hline \ell_4\, g_{k,x} & 0 & 0 \\ 0 & \ell_4\, g_{k,y} & 0 \\ 0 & 0 & \ell_4\, g_{k,z} \\ \frac{1}{\sqrt{2}}\, \ell_4\, g_{k,y} & \frac{1}{\sqrt{2}}\, \ell_4\, g_{k,x} & 0 \\ \frac{1}{\sqrt{2}}\, \ell_4\, g_{k,z} & 0 & \frac{1}{\sqrt{2}}\, \ell_4\, g_{k,x} \\ 0 & \frac{1}{\sqrt{2}}\, \ell_4\, g_{k,z} & \frac{1}{\sqrt{2}}\, \ell_4\, g_{k,y} \\ \hline 0_{6\times 1} & 0_{6\times 1} & 0_{6\times 1} \end{array}\right] d\beta \in I\!R^{30\times 3} \tag{98}$$

5.2.5 Elastic relation for the element

Considering the m and n matrices as defined in Eqs. (62) and (64) the following discrete elastic relation can be written in terms of the global vector of stress parameters

$$\boldsymbol{N}_\sigma^T \mathbb{E}^{-1} \boldsymbol{N}_\sigma = \begin{bmatrix} \ell_1^2 n & \ell_1\ell_2 n & \ell_1\ell_3 n & \ell_1\ell_4 n & 0_{6\times6} \\ \ell_1\ell_2 n & \ell_2^2 n & \ell_2\ell_3 n & \ell_2\ell_4 n & 0_{6\times6} \\ \ell_1\ell_3 n & \ell_2\ell_3 n & \ell_3^2 n & \ell_3\ell_4 n & 0_{6\times6} \\ \ell_1\ell_4 n & \ell_2\ell_4 n & \ell_3\ell_4 n & \ell_4^2 n & 0_{6\times6} \\ 0_{6\times6} & 0_{6\times6} & 0_{6\times6} & 0_{6\times6} & \frac{1}{h} n \end{bmatrix} \in \mathbb{R}^{30\times30} \tag{99}$$

$$\mathbb{E}^{-1^e} = \int_{\beta^e} \boldsymbol{N}_\sigma^T \mathbb{E}^{-1} \boldsymbol{N}_\sigma \; d\beta \in \mathbb{R}^{30\times30} \tag{100}$$

Calculating the matrix a such that

$$a^{-1} := \int_{\beta^e} \begin{bmatrix} \ell_1^2 & \ell_1\ell_2 & \ell_1\ell_3 & \ell_1\ell_4 \\ \ell_1\ell_2 & \ell_2^2 & \ell_2\ell_3 & \ell_2\ell_4 \\ \ell_1\ell_3 & \ell_2\ell_3 & \ell_3^2 & \ell_3\ell_4 \\ \ell_1\ell_4 & \ell_2\ell_4 & \ell_3\ell_4 & \ell_4^2 \end{bmatrix} d\beta \in \mathbb{R}^{4\times4} \tag{101}$$

and being β^e the element volume we have:

$$\mathbb{E}^{-1^e} = \begin{bmatrix} a_{11} n & a_{12} n & a_{13} n & a_{14} n & 0_{6\times6} \\ a_{21} n & a_{22} n & a_{23} n & a_{24} n & 0_{6\times6} \\ a_{31} n & a_{32} n & a_{33} n & a_{34} n & 0_{6\times6} \\ a_{41} n & a_{42} n & a_{43} n & a_{44} n & 0_{6\times6} \\ 0_{6\times6} & 0_{6\times6} & 0_{6\times6} & 0_{6\times6} & \frac{\beta^e}{h} n \end{bmatrix} \in \mathbb{R}^{30\times30} \tag{102}$$

The coefficients of $\mathbb{E}^{-1^e}$ are obtained by integration considering a quadratic mapping of the geometry. Obtained the matrix $\mathbb{E}^{-1^e}$ the matrix $\mathbb{E}^e$ can be obtained by direct inversion, taking advantage of the uncoupling between the coefficients matrices a_{ij} and $\frac{\Omega^e}{h}$.

$$\mathbb{E}^e = \begin{bmatrix} a_{11} m & a_{12} m & a_{13} m & a_{14} m & 0_{6\times6} \\ a_{21} m & a_{22} m & a_{23} m & a_{24} m & 0_{6\times6} \\ a_{31} m & a_{32} m & a_{33} m & a_{34} m & 0_{6\times6} \\ a_{41} m & a_{42} m & a_{43} m & a_{44} m & 0_{6\times6} \\ 0_{6\times6} & 0_{6\times6} & 0_{6\times6} & 0_{6\times6} & \frac{h}{\beta^e} m \end{bmatrix} \in \mathbb{R}^{30\times30} \tag{103}$$

5.2.6 Discrete thermal deformation

$$\theta^n = \begin{bmatrix} \theta^1 & \dots & \theta^{10} \end{bmatrix} \in \mathbb{R}^{10} \tag{104}$$

$$\theta^e = \sum g_j \, \theta^j \tag{105}$$

$$\Theta^n = \begin{bmatrix} \alpha \sum g_j \, \theta^j \\ \alpha \sum g_j \, \theta^j \\ \alpha \sum g_j \, \theta^j \\ 0_{3\times1} \end{bmatrix} \tag{106}$$

$$\mathbf{\Theta}^e = \int_{\beta^e} \begin{bmatrix} \alpha\,\ell_1 \sum g_j\,\theta^j \\ \alpha\,\ell_1 \sum g_j\,\theta^j \\ \alpha\,\ell_1 \sum g_j\,\theta^j \\ 0_{3\times1} \\ \alpha\,\ell_2 \sum g_j\,\theta^j \\ \alpha\,\ell_2 \sum g_j\,\theta^j \\ \alpha\,\ell_2 \sum g_j\,\theta^j \\ 0_{3\times1} \\ \alpha\,\ell_3 \sum g_j\,\theta^j \\ \alpha\,\ell_3 \sum g_j\,\theta^j \\ \alpha\,\ell_3 \sum g_j\,\theta^j \\ 0_{3\times1} \\ \alpha\,\ell_4 \sum g_j\,\theta^j \\ \alpha\,\ell_4 \sum g_j\,\theta^j \\ \alpha\,\ell_4 \sum g_j\,\theta^j \\ 0_{3\times1} \end{bmatrix} d\beta \in I\!R^{30} \tag{107}$$

5.3 Stein's model - discretization of yield functions and their gradients and Hessians

For each one of the fours stress nodes, two yield modes exists corresponding to the yield surfaces of the Stein's model. Thus, in the element, eight yield modes have to be considered.

5.3.1 Yield modes

For k varying from 1 to 4

$$f_{S1}^{(k)} = (\sigma_x^{(k)} - A_x)^2 + (\sigma_y^{(k)} - A_y)^2 + (\sigma_z^{(k)} - A_z)^2 - (\sigma_x^{(k)} - A_x)(\sigma_y^{(k)} - A_y) \tag{108}$$

$$- (\sigma_x^{(k)} - A_x)(\sigma_z^{(k)} - A_z) - (\sigma_y^{(k)} - A_y)(\sigma_z^{(k)} - A_z) \tag{109}$$

$$+\frac{3}{2}(\sigma_{(xy)}^{(k)} - A_{(xy)})^2 + \frac{3}{2}(\sigma_{(xz)}^{(k)} - A_{(xz)})^2 + \frac{3}{2}(\sigma_{(yz)}^{(k)} - A_{(yz)})^2 \tag{110}$$

$$- \sigma_{Y0}^2 \tag{111}$$

$$f_{S2}^{(k)} = A_x^2 + A_y^2 + A_z^2 - A_xA_y - A_xA_z - A_yA_z + \frac{3}{2}A_{(xy)}^2 + \frac{3}{2}A_{(xz)}^2 + \frac{3}{2}A_{(yz)}^2 \tag{112}$$

$$- (\sigma_Y - \sigma_{Y0})^2 \tag{113}$$

5.3.2 Gradients

Defining $G1$, $G2$ and $G3$ matrix as below:

$$G1 = \begin{bmatrix} 2(\sigma_x^{(1)} - A_x) - (\sigma_y^{(1)} - A_y) - (\sigma_z^{(1)} - A_z) \\ 2(\sigma_y^{(1)} - A_y) - (\sigma_x^{(1)} - A_x) - (\sigma_z^{(1)} - A_z) \\ 2(\sigma_z^{(1)} - A_z) - (\sigma_x^{(1)} - A_x) - (\sigma_y^{(1)} - A_y) \\ 3(\sigma_{(xy)}^{(1)} - A_{(xy)}) \\ 3(\sigma_{(xz)}^{(1)} - A_{(xz)}) \\ 3(\sigma_{(yz)}^{(1)} - A_{(yz)}) \end{bmatrix} \tag{114}$$

$$G2 = \begin{bmatrix} -2(\sigma_x^{(1)} - A_x) + (\sigma_y^{(1)} - A_y) + (\sigma_z^{(1)} - A_z) \\ -2(\sigma_y^{(1)} - A_y) + (\sigma_x^{(1)} - A_x) + (\sigma_z^{(1)} - A_z) \\ -2(\sigma_z^{(1)} - A_z) + (\sigma_x^{(1)} - A_x) + (\sigma_y^{(1)} - A_y) \\ -3(\sigma_{(xy)}^{(1)} - A_{(xy)}) \\ -3(\sigma_{(xz)}^{(1)} - A_{(xz)}) \\ -3(\sigma_{(yz)}^{(1)} - A_{(yz)}) \end{bmatrix} \tag{115}$$

and

$$G3 = \begin{bmatrix} 2A_x - A_y - A_z \\ 2A_y - A_x - A_z \\ 2A_z - A_x - A_y \\ 3A_{(xy)} \\ 3A_{(xz)} \\ 3A_{(yz)} \end{bmatrix} \tag{116}$$

The components of the gradient in each stress nodes are:

Node 1

$$\nabla_\sigma f_{S1}^{(1)} = \begin{bmatrix} G1 \\ 0_{18\times1} \\ G2 \end{bmatrix} \tag{117}$$

$$\nabla_\sigma f_{S2}^{(1)} = \begin{bmatrix} 0_{24\times1} \\ G3 \end{bmatrix} \tag{118}$$

Node 2

$$\nabla_\sigma f_{S1}^{(2)} = \begin{bmatrix} 0_{6\times1} \\ G1 \\ 0_{12\times1} \\ G2 \end{bmatrix} \tag{119}$$

$$\nabla_\sigma f_{S2}^{(2)} = \begin{bmatrix} 0_{24\times1} \\ G3 \end{bmatrix} \tag{120}$$

Node 3

$$\nabla_\sigma f_{S1}^{(3)} = \begin{bmatrix} 0_{12\times1} \\ G1 \\ 0_{6\times1} \\ G2 \end{bmatrix} \tag{121}$$

$$\nabla_\sigma f_{S2}^{(3)} = \begin{bmatrix} 0_{24\times1} \\ G3 \end{bmatrix} \tag{122}$$

Node 4

$$\nabla_\sigma f_{S1}^{(4)} = \begin{bmatrix} 0_{18\times1} \\ G1 \\ G2 \end{bmatrix} \tag{123}$$

$$\nabla_\sigma f_{S2}^{(4)} = \begin{bmatrix} 0_{24\times1} \\ G3 \end{bmatrix} \tag{124}$$

5.3.3 Hessian discretization

Calling:

$$He = \begin{bmatrix} 2 & -1 & -1 & 0 & 0 & 0 \\ -1 & 2 & -1 & 0 & 0 & 0 \\ -1 & -1 & 2 & 0 & 0 & 0 \\ 0 & 0 & 0 & 3 & 0 & 0 \\ 0 & 0 & 0 & 0 & 3 & 0 \\ 0 & 0 & 0 & 0 & 0 & 3 \end{bmatrix} \tag{125}$$

$$\tag{126}$$

the Hessian matrix in the four stress nodes are written:

$$\tag{127}$$

Node 1

$$\nabla_{\sigma\sigma} f_{S1}^{(1)} = \begin{bmatrix} He & 0_{6\times18} & -He \\ 0_{18\times6} & 0_{18\times18} & 0_{18\times6} \\ -He & 0_{6\times18} & He \end{bmatrix} \tag{128}$$

$$\nabla_{\sigma\sigma} f_{S2}^{(1)} = \begin{bmatrix} 0_{24\times24} & 0_{24\times6} \\ 0_{6\times24} & He \end{bmatrix} \tag{129}$$

$$\tag{130}$$

Node 2

$$\nabla_{\sigma\sigma} f_{S1}^{(2)} = \begin{bmatrix} 0_{6\times6} & 0_{6\times6} & 0_{6\times12} & 0_{6\times6} \\ 0_{6\times6} & He & 0_{6\times12} & -He \\ 0_{12\times6} & 0_{12\times6} & 0_{12\times12} & 0_{12\times6} \\ 0_{6\times6} & -He & 0_{6\times12} & He \end{bmatrix} \tag{131}$$

$$\nabla_{\sigma\sigma} f_{S2}^{(2)} = \begin{bmatrix} 0_{24\times24} & 0_{24\times6} \\ 0_{6\times24} & He \end{bmatrix} \tag{132}$$

$$\tag{133}$$

Node 3

$$\nabla_{\sigma\sigma} f_{S1}^{(3)} = \begin{bmatrix} 0_{12\times12} & 0_{12\times6} & 0_{12\times6} & 0_{12\times6} \\ 0_{6\times12} & He & 0_{6\times6} & -He \\ 0_{6\times12} & 0_{6\times6} & 0_{6\times6} & 0_{6\times6} \\ 0_{6\times12} & -He & 0_{6\times6} & He \end{bmatrix} \tag{134}$$

$$\nabla_{\sigma\sigma} f_{S2}^{(3)} = \begin{bmatrix} 0_{24\times24} & 0_{24\times6} \\ 0_{6\times24} & He \end{bmatrix} \tag{135}$$

$$\tag{136}$$

Node 4

$$\nabla_{\sigma\sigma} f_{S1}^{(4)} = \begin{bmatrix} 0_{18\times18} & 0_{18\times6} & 0_{18\times6} \\ 0_{6\times18} & He & -He \\ 0_{6\times18} & -He & He \end{bmatrix} \tag{137}$$

$$\nabla_{\sigma\sigma} f_{S2}^{(4)} = \begin{bmatrix} 0_{24\times24} & 0_{24\times6} \\ 0_{6\times24} & He \end{bmatrix} \tag{138}$$

6 APPLICATIONS

To verify the robustness and precision of this element in a 3D shakedown analysis, an application was done to a case with analytical solution. For the same case, a comparison between this 3D element with an axisymmetric one developed by Nery (2007) was done.

The example is a long closed pipe, subjected to internal pressure varying between zero and a maximum value $\overline{p}_{int}$. Independently, the pipe is subjected to a variable temperature field $\theta(R)$ with an instantaneous logarithm profile trough the wall. Let $\theta_{ext} = \theta_0 = 0$ be the external reference temperature and θ_{int} the internal temperature varying between θ_{ext} and a maximum value $\overline{\theta}_{int}$. The shakedown analytical solution was developed by Zouain and Silveira (2001) for ideal plasticity and by Nery (2007) for limited kinematic hardening.

6.1 Closed pipe under variable pressure and temperature loads

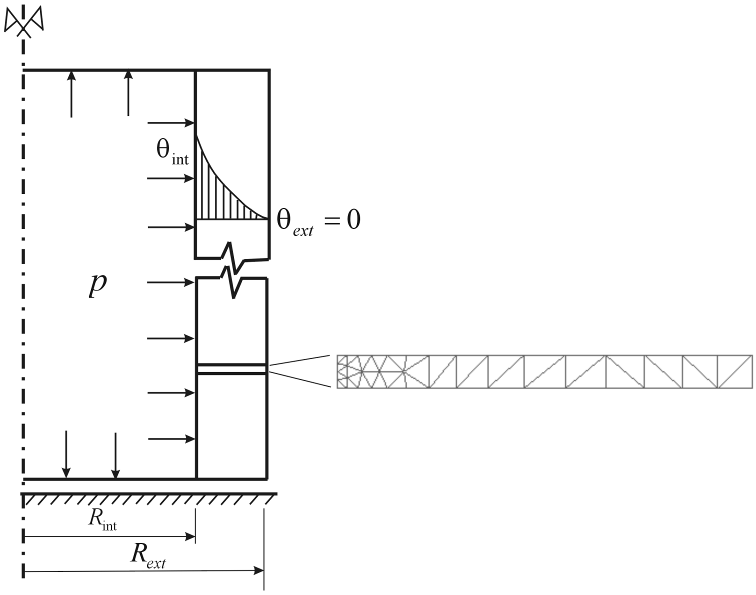

Figure 1: Free, long and closed pipe subject to independent variable pressure and thermal loads. The thermal load has a logarithmic profile through the wall. Is shown the 43 axisymmetric finite element mesh used in comparisons.

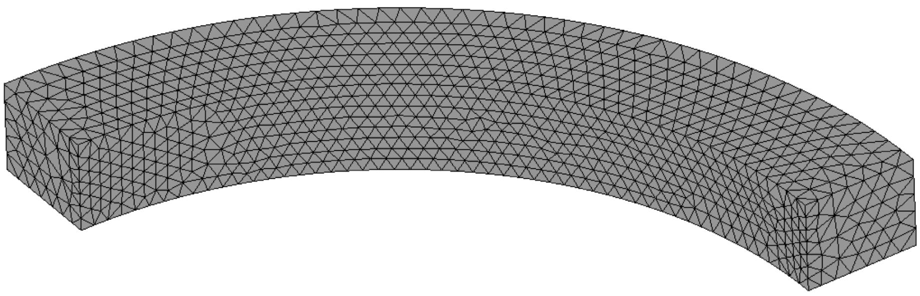

Figure 2: Tetrahedron 6232 elements mesh for the same example.

The internal and external radii of the tube are denoted by R_{int} and R_{ext}, respectively. We define a dimensionless radius

$$r := \frac{R}{R_{ext}} \tag{139}$$

that substitutes the radius R. Considering a dimensionless geometric parameter

$$\ell = \frac{R_{ext}}{R_{int}} \tag{140}$$

and a mechanical parameter

$$p := \frac{p_{int}}{(\ell^2 - 1)\sigma_Y} \tag{141}$$

where σ_Y is a yield stress at the end of hardening. Thus, p varies between zero and

$$\overline{p} = \frac{\overline{p}_{int}}{(\ell^2 - 1)\sigma_Y} \tag{142}$$

The collapse pressure of the closed pipe is:

$$p_c = \frac{2}{\sqrt{3}}\sigma_Y \ln \ell \tag{143}$$

We can define another parameter

$$\beta := \frac{\ell^2 - 1}{2\ln \ell} \tag{144}$$

and then, the mechanical load can be represented by:

$$\hat{p} := \frac{p_{int}}{p_c} = \sqrt{3}\beta p \tag{145}$$

varying between 0 e $\overline{\hat{p}} = \sqrt{3}\beta\overline{p}$.

The temperature profile θ through the wall as function of r is:

$$\theta(r) = \theta_{ext} - (\theta_{int} - \theta_{ext})\frac{\ln r}{\ln \ell} \tag{146}$$

To describe thermal stresses is used a dimensionless parameter

$$q := \frac{E\alpha_\theta(\theta_{int} - \theta_{ext})}{2(1-\nu)(\ell^2 - 1)\sigma_Y} \tag{147}$$

In dimensionless form, the limits of thermal load are zero and

$$\overline{q} := \frac{E\alpha_\theta\overline{\theta}}{2\sigma_Y(1-\nu)(\ell^2 - 1)} \tag{148}$$

Aiming to produce Bree-type diagrams as usually, a new dimensionless thermal parameter is defined:

$$\hat{q} := \frac{E\alpha_\theta(\theta_{int} - \theta_{ext})}{2(1-\nu)\sigma_Y} = (\ell^2 - 1)q \tag{149}$$

of which limits are zero and

$$\overline{\hat{q}} = (\ell^2 - 1)\overline{q} = \frac{E\alpha_\theta\overline{\theta}}{2\sigma_Y(1-\nu)} \tag{150}$$

The external loading is obtained by the solution of elastic stresses for a long, closed pipe: σ^p, under pressure only and σ^q under pure thermal load. This stress fields can be represented in dimensionless form using the reduced tensor

$$\tilde{\sigma} := (1/\sigma_Y)\sigma \tag{151}$$

Then:

$$\tilde{\sigma}^p := (1/p\sigma_Y)\sigma^p \qquad \tilde{\sigma}^q := (1/q\sigma_Y)\sigma^q \tag{152}$$

and the following variable loads are produced by elastic stresses:

$$\sigma^E = \sigma_Y(p\sigma^p + q\sigma^q) \tag{153}$$

where the basic elastic fields are defined in Zouain and Silveira (2001) and in Gokhfeld and Cherniavsky (1980).

The local domain of variable loads $\Delta(r)$ will be the parallelogram with four vertex $\{\tilde{\sigma}^k(r); k = 1:4\}$ defined by Eq.(153) with $(p,q) = \{(0,0),(0,\overline{q}),(\overline{p},\overline{q}),(\overline{p},0)\}$.

6.1.1 Analytical solution for alternating plasticity with hardening

Nery (2007) extend for limited kinematic hardening the work of Zouain and Silveira (2001) to obtain an analytical solution for the case when alternate plasticity occurs. The load amplifier factor ω satisfies the equation:

$$(\omega\bar{\hat{p}})^2\ell^4(\ell^2-1)^2 + 4(\omega\bar{\hat{q}})^2\beta^2(\ell^2-\beta)^2 + \\ 2\sqrt{3}(\omega\bar{\hat{p}})(\omega\bar{\hat{q}})\beta\ell^2(\ell^2-1)(\ell^2-\beta) = 4\beta^2(\ell^2-1)^2\left(\frac{\sigma_{Y0}}{\sigma_Y}\right)^2 \tag{154}$$

Plotted in a Bree-type diagram, as a function of the critical parameters defined in Eqs. (145) and (150), $(\hat{p},\hat{q}) = (\omega\bar{\hat{p}},\omega\bar{\hat{q}})$, this curve is an ellipse.

6.1.2 Analytical solution for incremental collapse

For elastic ideally-plastic materials, Zouain and Silveira (2001) finds an exact analytical solution from a simple mechanism of incremental collapse and beside this, an approximation with 0,6% error, which is the straight line defined by 155, with $\rho^{ub} \leq \mu$:

$$\rho^{ub}\bar{\hat{p}} + \frac{\sqrt{3}\beta\left[1-\beta(1-\ln\beta)\right]}{(\ell^2-1)^2}\rho^{ub}\bar{\hat{q}} = 1 \tag{155}$$

This results to be the same for limited kinematic material for incremental collapse.

6.1.3 Comparison between analytical and numerical solutions

Analytical and numerical values of 3D analysis for a pipe with relation $\ell := R_{ext}/R_{int} = 1.25$ are plotted in a Bree-type diagram, for elastic ideally-plastic (Zouain and Silveira, 2001), and for limited kinematical hardening materials, so that the comparisons can be made.

In figure (3) is shown the interaction Bree-type diagram for a long closed pipe, under independent thermal and pressure loads, in ideal plasticity $\sigma_{Y0}/\sigma_Y = 1.0$ and with kinematic hardening material with $\sigma_{Y0}/\sigma_Y = 0.8$. In this and in the following figure, the notation S indicates shakedown domain and E indicate the elastic domain. AP means alternate plasticity mechanism domain and IC means incremental collapse domain.

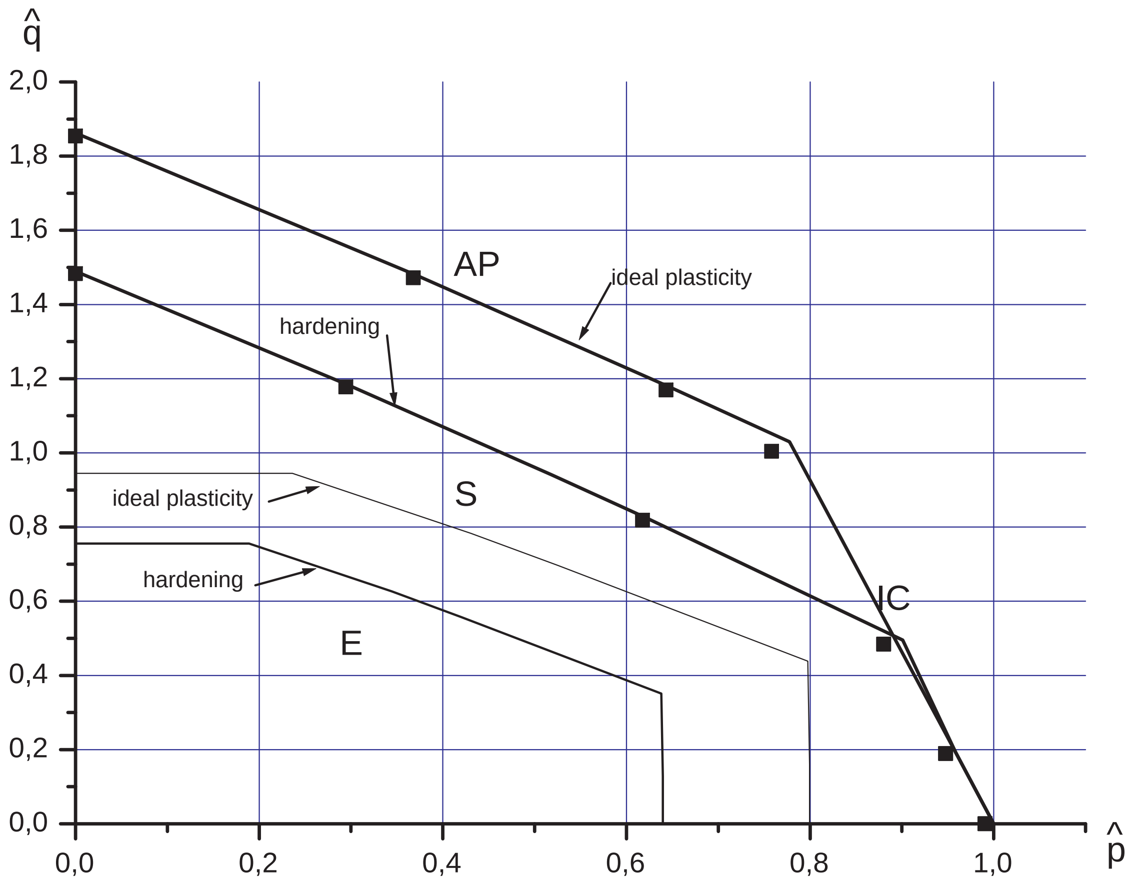

Figure 3: Interaction Bree-type diagram with the comparison between 3D analysis with 6232 tetrahedron elements (black squares) and analytical solution (lines) for a tube with thick wall $\ell = 1.25$ for ideal plasticity $\sigma_{Y0}/\sigma_Y = 1.0$ and for limited kinematic hardening with $\sigma_{Y0}/\sigma_Y = 0.8$.

6.1.4 Comparison between 3D and axisymmetrical numerical solutions

For the same example, the numerical results of the 3D shakedown analysis is compared with the numerical results of the axisymmetric one (Nery, 2007).

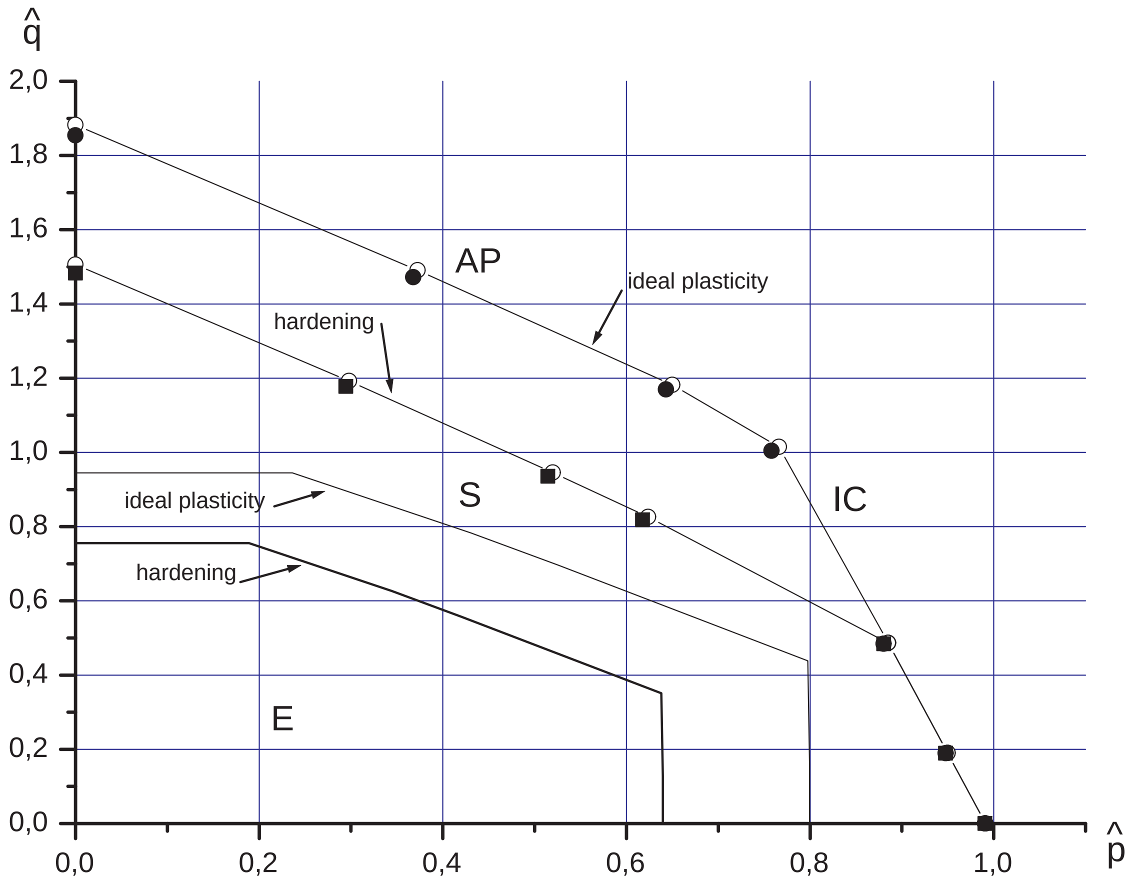

Figure 4: Interaction Bree-type diagram with the comparison between 3D analysis with 6232 tetrahedron elements (black squares) and axisymmetrical elements (hollow circles and lines) for a tube with thick wall $\ell = 1.25$ for ideal plasticity $\sigma_{Y0}/\sigma_Y = 1.0$ and for limited kinematic hardening with $\sigma_{Y0}/\sigma_Y = 0.8$.

7 CONCLUSION

In this work, the development of a mixed finite element to perform 3D shakedown analysis taking into account limited kinematic hardening materials was showed, extending the use of a available precise, efficient and robust algorithm developed originally for elastic ideally-plastic materials. This is in line with the current trend observed in a number of countries in which are involved universities, research centers and the industry searching for more realistic material properties in the 3D shakedown analysis. In industrial level, this important achievement permits to treat more complex components such as pipe bifurcations, valves and so on, aiming to assure their safety by the DBA analysis. Postulate defects in components also can be considered through a 3D analysis. Future developments should be made to enhance this element aiming to consider ductile plastic damage and the influence of temperature in the material properties to match the industrial demand for more realistic results.

8 ACKNOWLEDGEMENTS

The authors would like to acknowledge the financial support provided by CNPq and also to professor Néstor Zouain for making available the elastic ideally-plastic shakedown analysis source code without which this work would not have been possible.

REFERENCES

Gokhfeld D.A. and Cherniavsky D.F. *Limit analysis of structures at thermal cycling*. Sijthoff and Noordhoof, The Netherlands, 1980.

Halphen B. and Nguyen Q.S. Sur les matériaux standard généralisés. *Journal de Mécanique Théorique et Appliquée*, 14:1–37, 1975.

Lemaitre J. and Chaboche J.L. *Mechanics of solid materials*. Cambridge University Press, 1990.

Mackenzie D. and Boyle J. Pressure vessel design by analysis-a short course. SIBRAT, 1996.

Matt C.C. and Borges L. Formulação mista para termoelasticidade. *Proceedings of 22nd Iberian Latin American Congress on Computational methods in Engeneering- XXII CILAMCE*, 37:3323–3341, 2001.

Maugin G.A. *The Thermomechanics of Plasticity and Fracture*. Cambridge University Press, UK, 1992.

Nery D.E.S. *Estados limite de componentes mecânicos considerando encruamento cinemático limitado*. Ph.D. thesis, 2007.

Staat M. and Heitzer M. LISA – a European project for FEM-based limit and shakedown analysis. *Nuclear Engineering and Design*, 206:151–166, 2001.

Stein E., Zhang G., and Huang Y. Modeling and computation of shakedown problems for nonlinear hardening materials. *Computer Methods in Applied Mechanics and Engineering*, 103:247–272, 1993.

Stein E., Zhang G., and König J.A. Micromechanical modelling and computation of shakedown with nonlinear kinematic hardening including examples for 2-D problems. In D. Axelrad and W. Muschik, editors, *Recent Developments of Micromechanics*. 1990.

Stein E., Zhang G., and König J.A. Shakedown with nonlinear strain-hardening including structural computation using finite element method. *International Journal of Plasticity*, 8:1–31, 1992.

Zouain N. Shakedown and safety assessment. In E. Stein, R. de Borst, and T.J.R. Hughes, editors, *Encyclopedia of Computational Mechanics*, chapter 9, pages 291–334. John Wiley, 2004. ISBN 0-470-84699-2.

Zouain N., Borges L.A., and Silveira J.L. An algorithm for shakedown analysis with nonlinear yield functions. *Computer Methods in Applied Mechanics and Engineering*, 191(23-24):2463–2481, 2002.

Zouain N. and Silveira J.L. Bounds to shakedown loads. *International Journal of Solids and Structures*, 38(10-13):2249–2266, 2001.